Journal of Solid State Chemistry 183 (2010) 2144–2153

Contents lists available at ScienceDirect

Journal of Solid State Chemistry

journal homepage: www.elsevier.com/locate/jssc

Metal coordination architectures of N-propionyl-1-hydroxy-2-naphthoylhydrazide: From metalladiazamacrocycles to trinuclear complexes

Xuefeng Shi, Dacheng Li, Suna Wang*, Suyuan Zeng, Daqi Wang, Jianmin Dou*

School of Chemistry and Chemical Engineering, Liaocheng University, Liaocheng 252059, PR China

ARTICLE INFO

Article history:
Received 9 April 2010
Received in revised form
5 July 2010
Accepted 14 July 2010
Available online 17 July 2010

Keywords:
Naphthoylhydrazide
Metalladiazamacrocycle
Octanuclear
Hexanuclear
Trinuclear
Magnetic properties

ABSTRACT

Two metalladiazamacrocycles, 24-membered octanuclear $[Mn_8(pnhz)_8(DMF)_5(MeOH)_3]$2DMF 3.5MeOH (**1**) and 18-membered hexanuclear $[Fe_6(pnhz)_6(DMF)_6]$ (**2**), and two linear trinuclear complexes, $[Cu_3(pnhz)_2(Py)_6]$ 2Py (**3**) and $[Ni_3(pnhz)_2(Py)_4]$ (**4**), have been synthesized based on a trianionic pentadentate bridging ligand N-propionyl-1-hydroxy-2-naphthoylhydrazide (H_3pnhz). The complexes are characterized by elemental analysis, IR, UV–vis spectroscopy and single-crystal X-ray diffraction. The nature of metal ions and steric effect of N-propionyl-1-hydroxy-2-naphthoylhydrazide ligand play key roles in the formation of complexes with different nuclearity. Complexes **1**, **2** and **3** exhibit antiferromagnetic coupling interactions between the metal centers.

1. Introduction

Since the first metallacrown $[Mn^{III}_6(L)_6(MeOH)_6]$ with $[M–N–N]_n$ repeating units, known as metalladiazamacrocycle, had been synthesized using a pentadentate ligand (L=N-formyl-salicylhydrazide) by Lah's group in 1998 [1], metalladiazamacrocycles have attracted considerable attention due to their diverse molecular structures [2,3] and the extensive functions, such as molecular recognition [4], catalysis [5], microporous materials as gas storage and separation [6,7], bioactivity [8–10], along with the potential applications in magnetic properties [11–13] and supramolecular building blocks for the construction of metal-organic frameworks [6,7,14–17]. As a class of pentadentate ligand, N-acyl-salicylhydrazide can coordinate with trivalent metal ions, such as Mn(III) [18–20], Fe(III) [21], Co(III) [22,23] and Ga(III) [23,24], forming various nuclearities ranging from 18-membered to 60-membered metalladiazamacrocycles [18–30]. Both the metal ions and the N-acyl ligands have influences on the resulting structures. For example, the ring size and nuclearity of the metalladiazamacrocycles can be modified by controlling the steric hindrance and the rigidity of the N-acyl side chains. Substitution at the Cβ position of the N-acyl side chain resulted in 18-membered hexanuclear systems, while the introduction of Cα substituents caused the expansion of the ring to yield 24-membered octanuclear or 30-membered decanuclear systems. Comparably, when binding to divalent metal ions, such as Ni(II), Cu(II) and Zn(II), linear/nonlinear trinuclear and hexanuclear structures are inclined to be formed [31–37].

Meanwhile, only recent increasing attention is being paid to similar ligands of N-acyl-3-hydroxy-2-naphthoylhydrazide by substituting 3-hydroxy-2-naphthoyl group for salicyl group, and limited examples of Mn(III) and Ga(III) metalladiazamacrocycles have been reported [38–40]. We have obtained 30-membered decanuclear and 18-membered hexanuclear metalladiazamacrocycles based on a series of ligands, such as N-phenyl-3-hydroxy-2-naphthoylhydrazide (H_3bznhz), N-acetyl-3-hydroxy-2-naphthoylhydrazide (H_3anhz) and N-propionyl-3-hydroxy-2-naphthoylhydrazide (H_3pnhz) [39,40]. As part of our work to develop a better understanding of the effect of the metal centers and N-acyl ligands on the nuclearity of metallacrocyles and their properties, we synthesized a pentadentate ligand N-propionyl-1-hydroxy-2-naphthoylhydrazide (H_3pnhz) and four new complexes: two metalladiazamacrocycles, 24-membered octanuclear $[Mn_8(pnhz)_8(DMF)_5(MeOH)_3]\cdot 2DMF\cdot 3.5MeOH$ (**1**) and 18-membered hexanuclear $[Fe_6(pnhz)_6(DMF)_6]$ (**2**), and two linear trinuclear complexes, $[Cu_3(pnhz)_2(Py)_6]\cdot 2py$ (**3**) and $[Ni_3(pnhz)_2(Py)_8]$ (**4**). Measurements of the magnetic properties of **1**, **2** and **3** indicate that they exhibit antiferromagnetic coupling interactions between the metal centers.

2. Experimental section

2.1. Materials and instrumentation

All reagents and solvents are commercially available and used without further purification. Infrared spectra were recorded

* Corresponding authors. Fax: +86 0635 8239001.
E-mail addresses: wangsuna@lcu.edu.cn (S. Wang), jmdou@lcu.edu.cn (J. Dou).

0022-4596/$ - see front matter © 2010 Elsevier Inc. All rights reserved.
doi:10.1016/j.jssc.2010.07.021

on a Nicolet-5700 FT-IR spectrophotometer in the range 400–4000 cm^{-1} using KBr pellets. Elemental analysis (C, H and N) was carried out with a Perkin-Elmer 2400 II elemental analyzer. ^1H and ^{13}C NMR spectra were obtained on a Varian Mercury Plus 400 MHz NMR spectrometer. UV–visible spectral was performed on HP-8453 UV–vis spectrophotometer in DMF for complexes
1–4. Magnetic measurements were carried out on a Quantum Design MPMS-5XL SQUID system.

2.2. Syntheses

2.2.1. N-propionyl-1-hydoxy-2-naphthoylhydrazide (H_3pnhz)

An amount of 0.922 g (10 mmol) of propionyl chloride was added dropwise to a stirred solution of chloroform (70 ml) containing 0.741 g (10 mmol) of propionic acid and 1.012 g (10 mmol) of triethylamine at 0 °C. The stirring was continued for 1.5 h, and the solution was slowly warmed to ambient temperature. Then an amount of 2.02 g (10 mmol) of 1-hydoxy-2-naphthoylhydrazide was added to the mixture, with stirring being continued for another 24 h. After staying overnight in the refrigerator, the resulting white precipitate was filtered and washed with chloroform and diethyl ether, then dried in vacuo, 85% yield, Mp:154–157°. Anal. Calc. for $C_{14}H_{14}N_2O_3$: C 65.10%, H 5.46%, N 10.85%. Found: C 65.84%, H 5.20%, N 10.64%. ^1H NMR(DMSO-d_6, ppm): 13.79(s, 1H, Ar–OH), 10.65(s, 1H, Ar–CO–NH–), 9.93(s, 1H, C_2H_5–CO–NH–), 7.3–7.9(m, 6H, naphthalene ring), 3.56(s, 2H, –CH_2–), 1.15(t, 3H, –CH_3); ^{13}C NMR(DMSO-d_6, ppm): 172.38, 169.65, 159.72, 135.73, 128.54, 127.02, 125.28, 124.52, 117.51, 105.47, 78.37, 39.87, 26.46, 9.35. IR (KBr pellet): 3434(m), 3265(s), 3054(s), 2984(m), 1682(m), 1637(m), 1614(s), 1598(s), 1522(s), 1502(s), 1467(s), 1414(s), 1393(s), 1343(s), 1297(m), 1274(m), 1210(m), 1128(m), 1085(m), 1025(m), 945(m), 880(m), 787(m), 766(m)cm^{-1}.

2.2.2. $[Mn_8(pnhz)_8(DMF)_5(MeOH)_3]\cdot 2DMF\cdot 3.5MeOH$ (**1**)

An amount of 27.5 mg (0.1 mmol) of H_3pnhz and 0.3 mmol triethylamine were dissolved in 10 ml DMF and 24.5 mg (0.1 mmol) of manganese (II) acetate tetrahydrate were dissolved in 10 ml MeOH. The two solutions were mixed and stirred for 3 h. The resulting solution was allowed to stand for 20 days, whereupon dark red crystals were obtained in 74% yield, mp > 300°. Anal. Calc. for $C_{139.5}H_{161}Mn_8N_{23}O_{37.5}$: C 52.37%, H 5.07%, N 10.07%. Found: C 52.74%, H 4.67%, N 10.41%. IR(KBr pellet): 3056(m), 2973(m), 2935(m), 1657(s), 1617(m), 1597(m), 1562(m), 1513(m), 1483(m), 1453(s), 1430(m), 1415(m), 1402(m), 1378(m), 1359(m), 1261(m), 1222(m), 1145(m), 1102(m), 1063(m), 1025(m), 889(m), 760(m), 682(m), 617(m), 549(m), 519 (m), 440(m) cm^{-1}.UV: 209 (1.146), 252 (0.276), 273 (0.425), 303 (0.134), 334 (0.131)nm.

2.2.3. $[Fe_6(pnhz)_6(DMF)_6]$ (**2**)

An amount of 27.5 mg (0.1 mmol) of H_3pnhz was dissolved in 10 ml DMF, and 40.4 mg (0.1 mmol) of iron(III) nitrate monohydrate were dissolved in 10 ml MeOH. The later solution was dropped slowly into the former. Then the combined solution was allowed to stand still for one week, whereupon red crystals were obtained in 47% yield, mp > 300°. Anal. Calc. for $C_{103}H_{112}Fe_6N_{18}O_{25}$: C 53.01%, H 4.80%, N 10.81%. Found: C 53.29%, H 4.46%, N 10.40%. IR(KBr pellet): 2968(m), 2938(m), 1651(s), 1561(s), 1529(m), 1514(m), 1479(s), 1450(m), 1406(s), 1381(m), 1385(s), 1307(m), 1262(m), 1229(m), 1144(m), 1105(m), 1027(m), 888(m), 833(m), 796(m), 765(m), 739(m), 658(m), 579(m), 519(m), 469(m) cm^{-1}. UV: 208 (0.422), 230 (0.7), 262 (0.884), 288 (0.621), 307 (0.84)nm.

2.2.4. $[Cu_3(pnhz)_2(Py)_6]\cdot 2Py$ (**3**)

An amount of 27.5 mg (0.1 mmol) of H_3pnhz was dissolved in 10 ml Py and 29.9 mg (0.15 mmol) of copper acetate was dissolved in 10 ml DMF. The two solutions were mixed together and stirred for 3 h. The resulting solution was allowed to stand still for 10 days, whereupon green crystals were obtained in 66% yield, mp > 300°C. Anal. Calc. for $C_{68}H_{62}Cu_3N_{12}O_6$: C, 61.75%; H, 4.34%; N, 12.29%. Found: C, 61.22%; H, 4.68%; N, 12.6%. IR (KBr pellet): 2966(m), 2933(m), 1609(m), 1569(s), 1543(m), 1522(s), 1486(m), 1449(s), 1413(s), 1388(m), 1360(m), 1310(m), 1259(s), 1219(m), 1102(m), 1072(m), 1043(m), 882(m), 846(m), 788(m), 754(s), 694(s), 669(m), 634(m), 578(m), 464(m) cm^{-1}. UV: 218 (0.206), 268 (0.156), 312 (1.048), 359 (1.087)nm.

2.2.5. $[Ni_3(pnhz)_2(Py)_4]$ (**4**)

Complex **4** was prepared in an analogous manner to that used for the complex **3**: using a 37.3 mg (0.15 mmol) of nickel (II) acetate tetrahydrate in 10 ml Py. Red crystals were obtained in 75% yield, mp > 300 °C. Anal. Calc. for $C_{48}H_{42}N_8Ni_3O_6$: C, 57.14%; H, 4.50%; N, 11.51%. Found: C, 57.48%; H, 4.22%; N, 11.17%. IR (KBr pellet): 2968(m), 2933(m), 1616(m), 1600(m), 1566(s), 1526(s), 1485(m), 1450(s), 1428(m), 1416(m), 1381(m), 1365(m), 1316(m), 1263(m), 1214(m), 1142(m), 1107(m), 1071(m), 1029(m), 890(m), 846(m), 812(m), 791(m), 759(s), 694(s), 614(m), 579(m), 521(m), 453(m) cm^{-1}. UV: 204 (1.146), 229 (0.276), 254 (0.452), 321 (2.91)nm.

2.3. Crystallographic details and data

X-ray single-crystal diffraction data for the complexes **1–4** were collected on a Bruker SMART 1000 CCD diffractometer at 298 K with Mo-$K\alpha$ radiation ($\lambda = 0.71069$ Å). Semiempirical absorption corrections were applied following the procedure Sadabs [41]. The structures were solved by direct methods using the Shelxl-97 program of the Shelxtl package and refined with Shelxl [42]. All non-hydrogen atoms were refined anisotropically by full-matrix least squares calculations on F^2 using SHELXTL program package. Hydrogen atoms were placed geometrically and with U_{iso} constrained to be 1.2 (1.5 for methyl groups and hydroxy) times U_{eq} of the carrier atom. Crystal data collection and structure refinement parameters are listed in Tables 1 and 2, respectively.

3. Results and discussion

3.1. Spectral characterization

Strong intensive bands can be observed at 3434 and 3265 cm^{-1} for the ligand, which can be attributed to stretching vibration of ν(O–H) phenolic and ν(N–H), respectively. There is a medium intensive band at 1682 cm^{-1} and a strong intensive band at 1637 cm^{-1} belonging to ν(C=O) and ν(C=N–N=C), respectively [43–47]. Bands at 1231–1225 cm^{-1} is assigned to the stretching vibration of ν(Ph–O). In the complexes, the absence of the N–H vibration bands at 3265 cm^{-1} is consistent with the deprotonation of N–H group and coordination to the metal ions; the presence of the bands at 1358 and 1261 cm^{-1} supported the involvement of phenolic oxygen in coordination through deprotonation. The deprotonation and coordination can also be confirmed by the band at 563–686 and 419–626 cm^{-1}, which were assigned to M–O and M–N linkages, respectively [48–50].

Table 1
Crystal data collection and structure refinement parameters for complexes **1**–**4**.

Complex	**1**	**2**	**3**	**4**
Empirical formula	$C_{139.5}H_{161}Mn_8N_{23}O_{37.5}$	$C_{102}H_{108}Fe_6N_{18}O_{24}$	$C_{68}H_{62}Cu_3N_{12}O_6$	$C_{48}H_{42}N_8Ni_3O_6$
Formula weight	3199.4	2305.16	1333.92	1003.03
Crystal size (mm)	$0.49 \times 0.47 \times 0.33$	$0.43 \times 0.40 \times 0.32$	$0.49 \times 0.44 \times 0.43$	$0.45 \times 0.42 \times 0.36$
Crystal system	Triclinic	Monoclinic	Triclinic	Monoclinic
Space group	$P\bar{1}$	$P2(1)/n$	$P\bar{1}$	$P2(1)/c$
a (Å)	20.2445(19)	16.2783(18)	9.7429(9)	9.7596(19)
b (Å)	22.044(2)	20.886(2)	13.3243(16)	15.9028(16)
c (Å)	22.086(2)	17.6833(15)	13.4370(17)	14.7779(14)
α (deg.)	60.8490(10)	90	91.2580(10)	90
β (deg.)	73.483(2)	100.653(2)	101.545(2)	95.3530(10)
γ (deg.)	74.0480(10)	90	110.948(2)	90
Z	2	2	1	2
V (Å^3)	8142.3(14)	5908.6(10)	1587.7(3)	2283.6(5)
D_{calc} (mg/m^3)	1.305	0.789	1.395	1.459
μ (mm^{-1})	0.676	0.760	1.058	1.282
$F(000)$	3318	2388	689	1036
θ range (deg.)	1.37–25.02	1.52–25.01	1.55–25.02	1.89–25.01
Reflections collected	42418	29945	7892	11273
Nique reflections (R_{int})	28303(0.0489)	10262(0.0673)	5339(0.0336)	4028(0.0274)
Data/restraints/parameters	28303/0/1991	6237/14/413	5339/0/404	4028/0/362
Goodness-of-fit on F^2	1.000	1.006	1.000	1.000
R indices	$R_1=0.0882$	$R_1=0.0863$	$R_1=0.0500$	$R_1=0.0399$
$[I > 2\sigma(I)]$	$wR_2=0.2221$	$wR_2=0.2079$	$wR_2=0.1079$	$wR_2=0.1077$

Table 2
Bond lengths (Å) and angles (deg.) of complexes **1**–**4**.

Complex ***1***					
Mn(1)–O(2)	1.870(5)	Mn(1)–O(3)	1.928(5)	Mn(1)–N(1)	1.930(6)
Mn(1)–O(22)	1.958(5)	Mn(1)–O(25)	2.217(7)	Mn(1)–N(16)	2.239(7)
O(2)–Mn(1)–O(3)	170.2(2)	O(2)–Mn(1)–N(1)	90.0(2)	O(3)–Mn(1)–N(1)	80.2(2)
O(2)–Mn(1)–O(22)	96.8(2)	O(3)–Mn(1)–O(22)	93.0(2)	N(1)–Mn(1)–O(22)	172.4(2)
O(2)–Mn(1)–O(25)	88.8(3)	O(3)–Mn(1)–O(25)	91.3(2)	N(1)–Mn(1)–O(25)	91.0(3)
O(22)–Mn(1)–O(25)	85.6(2)	O(2)–Mn(1)–N(16)	90.6(2)	O(3)–Mn(1)–N(16)	92.5(2)
N(1)–Mn(1)–N(16)	108.6(2)	O(22)–Mn(1)–N(16)	74.9(2)	O(25)–Mn(1)–N(16)	160.4(2)
Complex ***2***					
Fe(1)–O(2)	1.918(5)	Fe(1)–O(4)	2.003(4)	Fe(1)–N(1)	2.048(5)
Fe(1)–O(3)	2.028(5)	Fe(1)–O(10)	2.044(6)	Fe(1)–N(4)	2.094(5)
O(2)–Fe(1)–O(4)	104.2(2)	O(2)–Fe(1)–O(3)	160.7(2)	O(3)–Fe(1)–N(1)	75.41(19)
O(4)–Fe(1)–O(3)	95.17(19)	O(2)–Fe(1)–O(10)	91.3(2)	O(10)–Fe(1)–N(1)	87.5(2)
O(4)–Fe(1)–O(10)	85.7(2)	O(3)–Fe(1)–O(10)	90.1(2)	O(2)–Fe(1)–N(4)	92.6(2)
O(2)–Fe(1)–N(1)	85.4(2)	O(4)–Fe(1)–N(1)	168.4(2)	O(4)–Fe(1)–N(4)	75.98(19)
O(3)–Fe(1)–N(4)	92.1(2)	O(10)–Fe(1)–N(4)	161.7(2)	N(1)–Fe(1)–N(4)	110.7(2)
Complex ***3***					
Cu(1)–O(1)	1.954(2)	Cu(2)–O(2)	1.925(2)	Cu(1)–N(2)	1.994(3)
Cu(1)–O(1)#1	1.954(2)	Cu(2)–O(3)	1.973(2)	Cu(2)–N(3)	2.378(4)
Cu(1)–N(2)#1	1.994(3)	Cu(2)–N(4)	2.044(3)	Cu(2)–N(1)	1.915(3)
O(1)–Cu(1)–O(1)#1	180.000(1)	O(2)–Cu(2)–O(3)	170.68(11)	N(1)–Cu(2)–O(2)	91.78(11)
O(1)–Cu(1)–N(2)#1	98.85(11)	N(1)–Cu(2)–N(4)	163.43(14)	O(3)–Cu(2)–N(3)	90.02(12)
O(1)#1–Cu(1)–N(2)#1	81.15(11)	O(2)–Cu(2)–N(4)	92.89(12)	N(1)–Cu(2)–O(3)	80.70(11)
O(1)–Cu(1)–N(2)	81.15(11)	O(3)–Cu(2)–N(4)	92.87(12)	N(4)–Cu(2)–N(3)	96.04(13)
O(1)#1–Cu(1)–N(2)	98.85(11)	N(1)–Cu(2)–N(3)	99.19(14)	O(2)–Cu(2)–N(3)	96.65(12)
N(2)#1–Cu(1)–N(2)	180.000(1)				
Complex ***4***					
Ni(1)–N(1)	1.821(3)	Ni(1)–N(3)	1.92(3)	Ni(1)–O(2)	1.826(3)
Ni(1)–O(3)	1.846(3)	Ni(1)–N(3')	1.93(6)	Ni(2)–O(1)	2.033(3)
Ni(2)–O(1)#1	2.033(3)	Ni(2)–N(2)#1	2.067(3)	Ni(2)–N(4)#1	2.165(4)
Ni(2)–N(4)	2.165(4)	Ni(2)–N(2)	2.067(3)		
N(1)–Ni(1)–O(2)	95.02(13)	O(1)–Ni(2)–N(2)	78.60(12)	O(1)–Ni(2)–O(1)#1	180.000(1)
N(1)–Ni(1)–O(3)	84.33(13)	O(1)#1–Ni(2)–N(2)	101.40(12)	O(1)–Ni(2)–N(2)#1	101.40(12)
O(2)–Ni(1)–O(3)	179.17(14)	N(2)#1–Ni(2)–N(2)	180.000(1)	O(1)#1–Ni(2)–N(2)#1	78.60(12)
N(1)–Ni(1)–N(3)	171.2(8)	O(1)–Ni(2)–N(4)	89.80(14)	N(2)#1–Ni(2)–N(4)#1	85.63(14)
O(2)–Ni(1)–N(3)	90.0(11)	O(1)#1–Ni(2)–N(4)	90.20(14)	N(2)–Ni(2)–N(4)#1	94.37(14)
O(3)–Ni(1)–N(3)	90.6(11)	N(2)#1–Ni(2)–N(4)	94.37(14)	N(4)–Ni(2)–N(4)#1	180.00(14)
N(1)–Ni(1)–N(3′)	170.9(13)	N(2)–Ni(2)–N(4)	85.63(14)	N(2)#1–Ni(2)–N(4)#1	85.63(14)
O(2)–Ni(1)–N(3′)	89(2)	O(1)–Ni(2)–N(4)#1	90.20(14)	O(1)#1–Ni(2)–N(4)#1	89.80(14)

Symmetry codes: for complex **3**, #1 $-x+2$, $-y+2$, $-z+2$; complex **4**, #1 $-x+2$, $-y$, $-z+2$.

3.2. Structure descriptions of complexes **1–4**

3.2.1. $[Mn_8(pnhz)_8(DMF)_5(MeOH)_3]\cdot 2DMF\cdot 3.5MeOH$ (**1**)

Complex $[Mn_8(pnhz)_8(DMF)_5(MeOH)_3]\cdot 2DMF\cdot 3.5MeOH$ (**1**) crystallized in the triclinic system with space group $P\bar{1}$. As shown in Fig. 1a, the asymmetric unit is composed of eight manganese atoms, eight triply-deprotonated $pnhz^{3-}$ ligands, five coordinated DMF molecules and three coordinated CH_3OH molecules as well as two uncoordinated DMF molecules and three uncoordinated CH_3OH molecules.

The triple-deprotonated pentadentate ligand has five potential coordination sites, involving two hydrazide nitrogen atoms, two carbonyl oxygen atoms and one phenol oxygen atom, in which the phenolate oxygen, one hydrazide nitrogen and one carbonyl oxygen can bond to one Mn(III) ion in the meridional mode to produce a 5-membered chelating ring and a 6-membered chelating ring, whilst the other hydrazide nitrogen and carbonyl oxygen can bridge adjacent Mn(III) ions in a back-to-back mode to produce another 5-membered chelating ring. As a result, this tridentate-bidentate binding mode of the ligand around the metal center forces the stereochemistry of the metal ions into a propeller configuration [1], and bridges neighboring Mn(III) ions to form a 24-membered octanuclear metalladiazamacrocycle with the [Mn–N–N] repeating units and the alternating ⋯ΛΔΛΔ⋯ chiral configurations. The average neighboring Mn⋯Mn distance is 4.87 Å. The Mn⋯Mn⋯Mn angles are ranging from 121.94° to 129.29°, which are close to the value of the interior angle in an *n*-octagon (135°). The naphthalene rings and propionyl groups pointed out and into the cavity, respectively. The four DMF molecules coordinated at the Mn(III) centers with Λ configuration are on one face of the metalladiazamacrocycle, and the remaining one DMF and three CH_3OH molecules coordinated at other Mn(III) centers with Δ configuration are on the other face. The two faces of each metalladiazamacrocycle molecule have opposite chiralities.

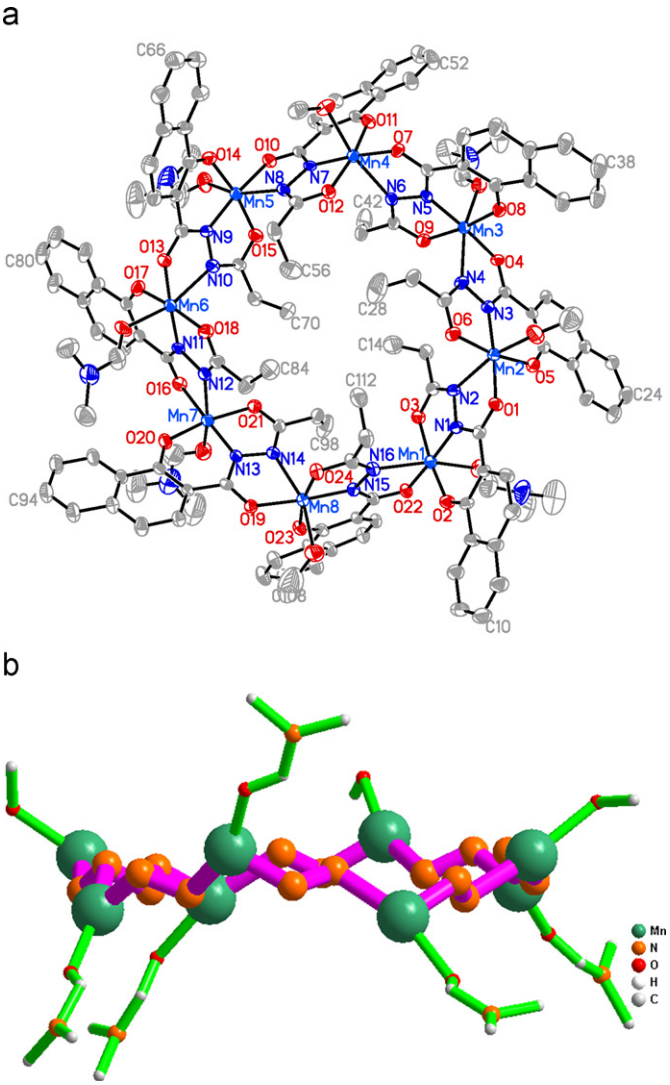

Fig. 1. (a) An ORTEP drawing of the structure of 24-metallacrown-8 of complex **1**. All hydrogen atoms have been omitted for clarity. (b) Sideview of the complex **1**, except the $[M–N–N–]_n$ unit and the coordinated DMF or CH_3OH molecules, other parts are omitted for clarity.

Each crown is measured about 21.99 Å in peripheral diameter (mean value of 21.23 Å for C52⋯C108, 22.53 Å for C38⋯C94, 22.92 Å for C24⋯C80 and 21.60 Å for C10⋯C66) and 8.39 Å in thickness (distance of $Cg_1\cdots Cg_2$ (Cg_1 is the center of four peripheral atoms of C38, C10, C66, C94 and Cg_2 is the center of C52, C108, C24, C80 atoms)) based on the farthest atoms without considering the van der Waals radii of the atoms, respectively. For the oval-shaped cavity, the approximate dimensions of the internal diameter at the entrance are 4.92 Å, measured between the opposite carbon atoms (C28, C56, C84, C112 and C14, C42, C70, C98) in the groups of the ligand. The largest distance of the opposite metal centers within the cavity is about 12.16 Å based on Mn1 and Mn5 centers.

All the manganese ions in the metalladiazamacrocycle are in a distorted octahedral MnO_4N_2 environment owing to the high-spin d^4 Mn(III) along *z*-axis elongated by the Jahn–Teller [25,38–40]. The bond distances of Mn–O (phenolate), Mn–O (carbonyl) and Mn–N (hydrazide) on the equatorial plane are in the range of 1.847(5)–1.979(6) Å, while the axial bond distances of Mn–N (hydrazide) and Mn–O (DMF or CH_3OH) are 2.217(7)–2.272(7) Å, respectively. Analysis of the supramolecular interactions indicates adjacent octanuclear units are constructed into 3D supramolecular architecture via C–H⋯π weak interactions between neighboring naphthalene rings and C–H⋯O interactions between the naphthalene ring and carbonyl oxygen atoms (Fig. 2 and Fig. S1) [51–54].

As far as we know, 18-membered hexanuclear manganese(III) metalladiazamacrocycles are common, especially for the unbranched N-acyl salicylhydrazides, such as N-propionyl-salicylhydrazide (H_3pshz) [55] and N-propionyl-5-chlorosalicylhydrazide (H_3pcshz) [43]. Comparably, only several 24-membered octanuclear manganese(III) metalladiazamacrocycles have been reported, all of which were induced by the introduction of Cα substituents into the N-acyl salicylhydrazide ligands, namely N-(2-methyl-propanoyl)salicylhydrazide ($H_3$2-mpshz) [28], N-isobutyryl-5-methylsalicylhydrazide (H_3ibumshz) [56], N-2-methyl-acryloyl-5-bromosalicylhydrazide [57], respectively. Herein, we reported a new 24-membered octanuclear metalladiazamacrocycles using N-propionyl-1-hydroxy-2-naphthaoylhydrazide. Except for the N-acylsubstituent groups, the sterically more demanding 3-hydroxy-2-naphthoyl group compared with salicyl group may also play an important role in expanding the nuclearity.

3.2.2. $[Fe_6(pnhz)_6(DMF)_6]$ (**2**)

Complex $[Fe_6(pnhz)_6(DMF)_6]$ (**2**) crystallized in the monoclinic system with space group $P2(1)/n$. As shown in Fig. 3 six Fe(III) centers, six deprotonated $pnhz^{3-}$ ligands and six coordinated DMF molecules construct an 18-membered hexanuclear metalladiazamacrocycle, with a crystallographic inversion center in the center of the cavity, similar to most known metalladiazamacrocycles. Both faces of the metalladiazamacrocycles have opposite chiralities with three DMF molecules on each face coordinating to the iron centers in Δ and Λ configurations, respectively. The average

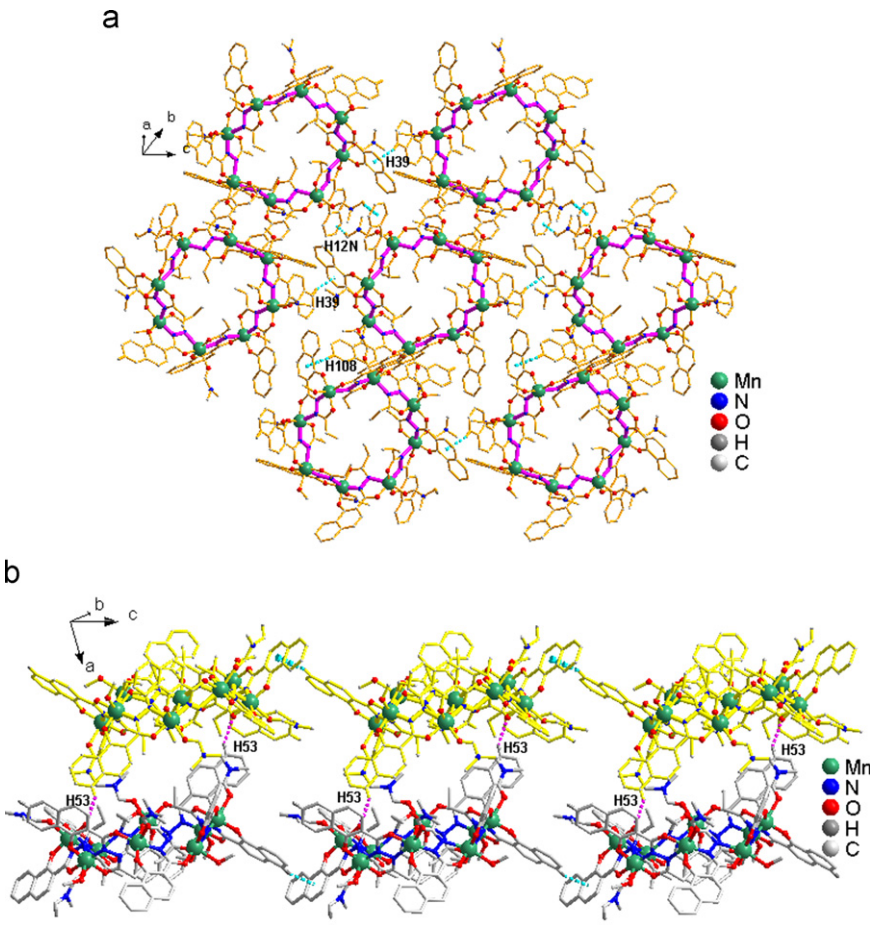

Fig. 2. (a) View of the 2D supramolecular structure of complex **1** linked by C–H···π interactions (dotted lines) between two naphthalene rings of adjacent molecules. (b) View of the 3D supramolecular structure linked by C–H···O interactions (dotted lines) between two naphthalene rings of adjacent molecules.

neighboring Fe···Fe atomic distance is 4.90 Å. The Fe···Fe···Fe interatomic angle are ranging from 108.56° to 125.18°, which is close to the value of the interior angle in an *n*-hexagon (120°). The triple-deprotonated ligand also exhibits tridentate–bidentate binding mode and each Fe(III) cation exhibits a distorted octahedral coordination environment by coordination of the DMF molecules. Compared with the MnN_2O_4 octahedron, there is no Jahn–Teller distortion in the FeN_2O_4 octahedron owing to the d^5 high-spin electronic configuration of the iron ion [11,44], and all the bond distances of Fe–O and Fe–N are in the range 1.907–2.137 Å.

Similarly, this complex is measured about 20.82 Å in peripheral diameter (mean value of 20.50 Å for C10···C10*A*, 21.61 Å for C38···C38*A*, 21.36 Å for C24···C24*A*) and 9.09 Å in thickness (distance of $Cg_1 \cdots Cg_2$ (Cg_1 is the center of three peripheral atoms of C10, C24, C38 and Cg2 is the center of C10*A*, C24*A*, C38*A*)) based on the farthest atoms without considering the van der Waals radii of the atoms, both values exceeding those of the previous $[Fe_6(pshz)_6(DMF)_6]$ [58] owing to the heavier head of 1-hydroxy-2-naphthyl groups. For the oval-shaped cavity, there are about 5.06 Å in the internal diameter at the entrance (measured between the opposite carbon atoms: C14, C28, C42 and C14*A*, C28*A*, C42*A*), about 9.68 Å (measured between the opposite metal atoms: Fe1 and Fe1*A*) at the center of the cavity and about 4.74 Å in depth of the cavity.

Adjacent molecules are constructed into 2D network (Fig. 4) via C23–H23···π (naphthalene ring C2–C7) stacking interactions with bond angle 134.37° and distance 3.207 Å.

3.2.3. $[Cu_3(pnhz)_2(Py)_6]\cdot 2py$ (**3**)

Different from the above complexes, complex $[Cu_3(pnhz)_2(Py)_6]\cdot 2py$ (**3**) is a linear trinuclear complex. As shown in Fig. 5, two triply-deprotonated pentadentate $pnhz^{3-}$ ligand bridge three metal ions in the same tridentate–bidentate binding mode, leading to a linear trinuclear unit with a Cu–N–N–Cu–N–N–Cu connectivity. Cu1, at the center of symmetry, adopts a distorted octahedral CuN_4O_2 coordination geometry with two carbonyl oxygen atoms, O1 and O1*A* (symmetry code: *A*, $-x+2$, $-y+2$, $-z+2$), two hydrazine nitrogen atoms, N2 and N2*A*, from two ligands. The axial positions are occupied by two pyridine molecules with a long Cu–N distance of 2.828 Å. The two terminal Cu(II) ions, Cu2 and Cu2*A*, are five-coordinated CuN_3O_2 tetragonal pyramidal geometry with phenolic oxygen, hydrazine nitrogen, carbonyl oxygen and pyridine nitrogen atoms in the equatorial plane and another pyridine nitrogen atom at the axial position. Adjacent metal ions Cu1 and Cu2 are separated with the distance of 4.63 Å. The Cu–O and Cu–N bond lengths are listed in Table 2.

These trinuclear units are constructed into 1D chains along the *a* axis via C–H···π interactions between C32 atoms of weak coordinated pyridine molecules and adjacent naphthalene ring (C2–C11) with H32···Cg (the center of C2–C7 ring) distance and C–H···Cg angle being 3.24 Å and 137.67°, respectively (Fig. 6).

3.2.4. $[Ni_3(pnhz)_2(Py)_8]$ (**4**)

Complex $[Ni_3(pnhz)_2(Py)_8]$ (**4**) is also a linear trinuclear complex similar to complex **3** (Figs.7 and 8) except that the two

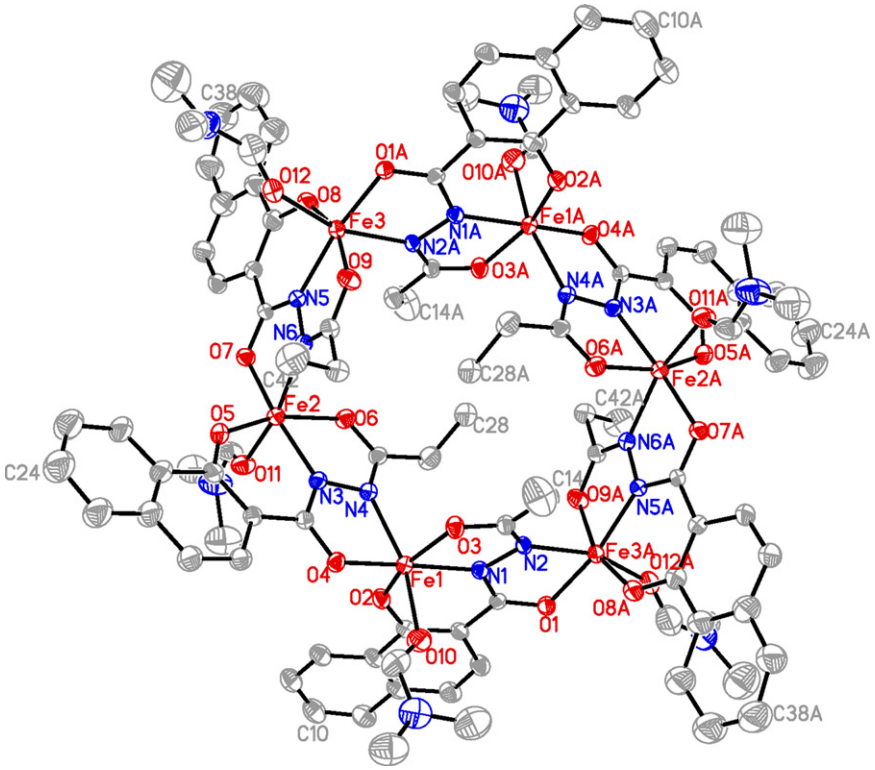

Fig. 3. An ORTEP drawing of the structure of 18-metallacrown-6 of complex **2**. All hydrogen atoms have been omitted for clarity. Symmetry code: *A*, 0.5 − *x*, 0.5 + *y*, 0.5 − *z*.

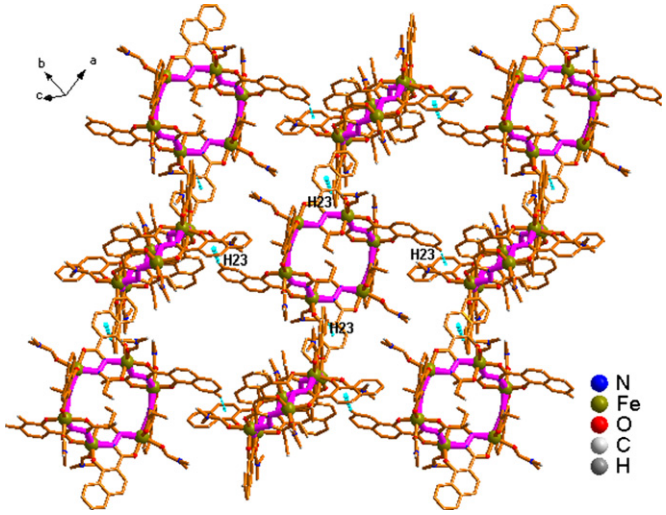

Fig. 4. View of the 2D supramolecular structure of complex **2** linked by C–H···π interactions (dotted lines) between two naphthalene rings of adjacent molecules.

terminal nickel(II) ions, Ni2 and Ni2A, adopt planar square geometry with one hydrazide nitrogen atom, one carbonyl oxygen atom, one phenolate oxygen atom and one nitrogen atom of pyridine. The bond distances of Ni–N (Py) are slightly longer than those of Ni–O (carbonyl) and Ni–N (hydrazide). The distance of $Ni_1 \cdots Ni_2$ is 4.61 Å. Adjacent units are also constructed into 1D chains via C22–H22···π (naphthalene ring C2–C7) stacking interactions. The bond angle between C22–H22 and the center of C2–C7 is 143.52° and the distance of C–H···π is 2.58 Å.

3.2.5. *Discussion of the structural diversity of all complexes of the N-acyl-3-hydroxy-2-naphthoylhydrazide ligand*

Based on N-propionyl-1-hydroxy-2-naphthoylhydrazide ligand, we have obtained four complexes with different nuclearity from octanuclear or hexanuclear metalladiazamacrocycles to simple linear trinuclear complexes (Scheme 1). To the best of our knowledge, for the N-acyl-3-hydroxy-2-naphthoylhydrazide system, only one 48-membered hexadecanuclear Mn(III) metalladiazamacrocyle, one 30-membered decanuclear Mn(III) metalladiazamacrocycles and three 18-membered hexanuclear Ga(III)/Mn(III) metalladiazamacrocycles have been reported [38–40]. For all the complexes, the ligand adopts tridentate-bidentate fashion to bridge the adjacent metal ions. Besides the nature of metal ions and the N-acyl-substituents which were commonly considered for N-acyl-salicylhydrazide system, the expansion of the nuclearity of the metalladiazamacrocyles could also be related to the sterically more demanding 3-hydroxy-2-naphthoyl group than salicyl group. Generally, for trivalent metal ions, Mn(III), Fe(III) and Ga(III), the octahedral coordination forces the stereochemistry of the metal ions into a propeller configuration and neighboring metal centers are connected to form 24- or 16-membered metalladiazamacrocyles with the [*M*–N–N] repeating units and the alternating ···ΛΔΛΔ··· chiral configurations. While for bivalent metal ions, Ni(II) and Cu(II) centers, the planar square or distorted tetragonal pyramidal geometry hinders the further connection between these center, only leading to linear trinuclear complexes with the limited unit of *M*–N–N–*M*–N–N–*M*. The similar conclusion had been made in a very recent reference, where it was based on a series of N-acylsubstituented salicylhydrazides and the steric effect of the N-acyl side chains

was also considered. Herein, we used a single ligand to verify this conclusion again. Additionally, for Mn(III) and Fe(III) complexes, the difference of the nucleariy may be related to the Jahn–Teller effect of the former. The longer bond length of axial positions of Mn(III) may decrease the steric hindrance and thus hold more atoms around the macrocycle.

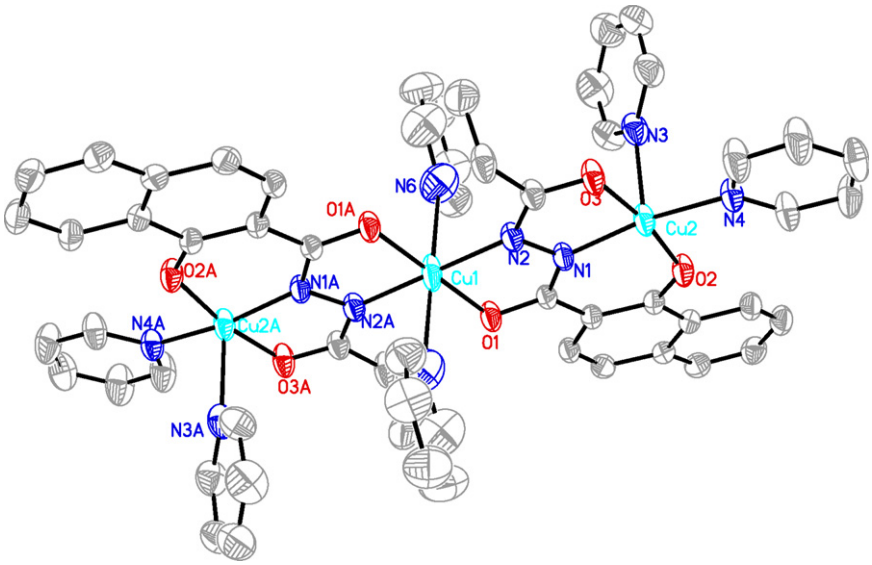

Fig. 5. An ORTEP drawing of the structure of trinuclear of complex **3**. All hydrogen atoms have been omitted for clarity. Symmetry code: *A*, $-x+2$, $-y+2$, $-z+2$.

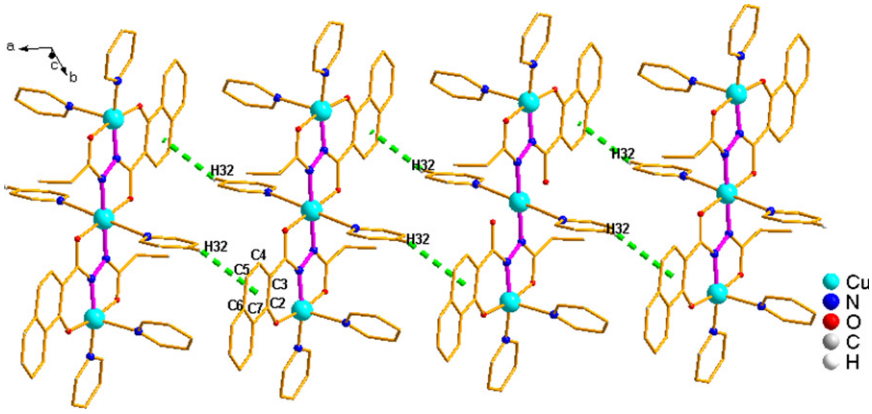

Fig. 6. View of the 1D supramolecular chain of complex **3** linked by C–H$\cdots\pi$ interactions (dotted lines) between the nitrogen pyridine molecules and naphthalene ring of adjacent trinuclear units.

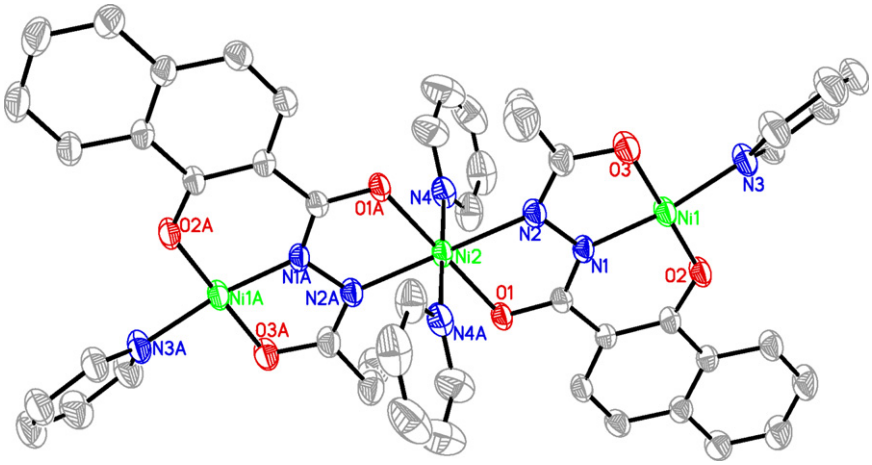

Fig. 7. An ORTEP drawing of the structure of trinuclear of complex **4**. All hydrogen atoms have been omitted for clarity. Symmetry code: *A*, $-x$, $0.5+y$, $0.5-z$.

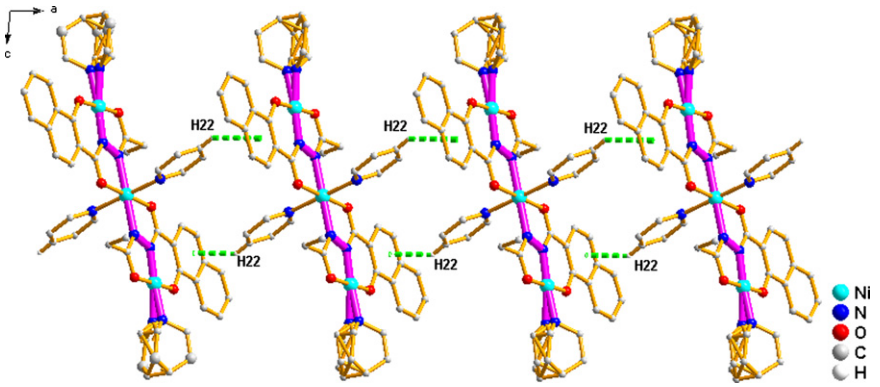

Fig. 8. View of the 1D supramolecular chain of complex **4** linked by C–H···π interactions (dotted lines) between the nitrogen pyridine molecules and naphthalene ring of adjacent trinuclear units.

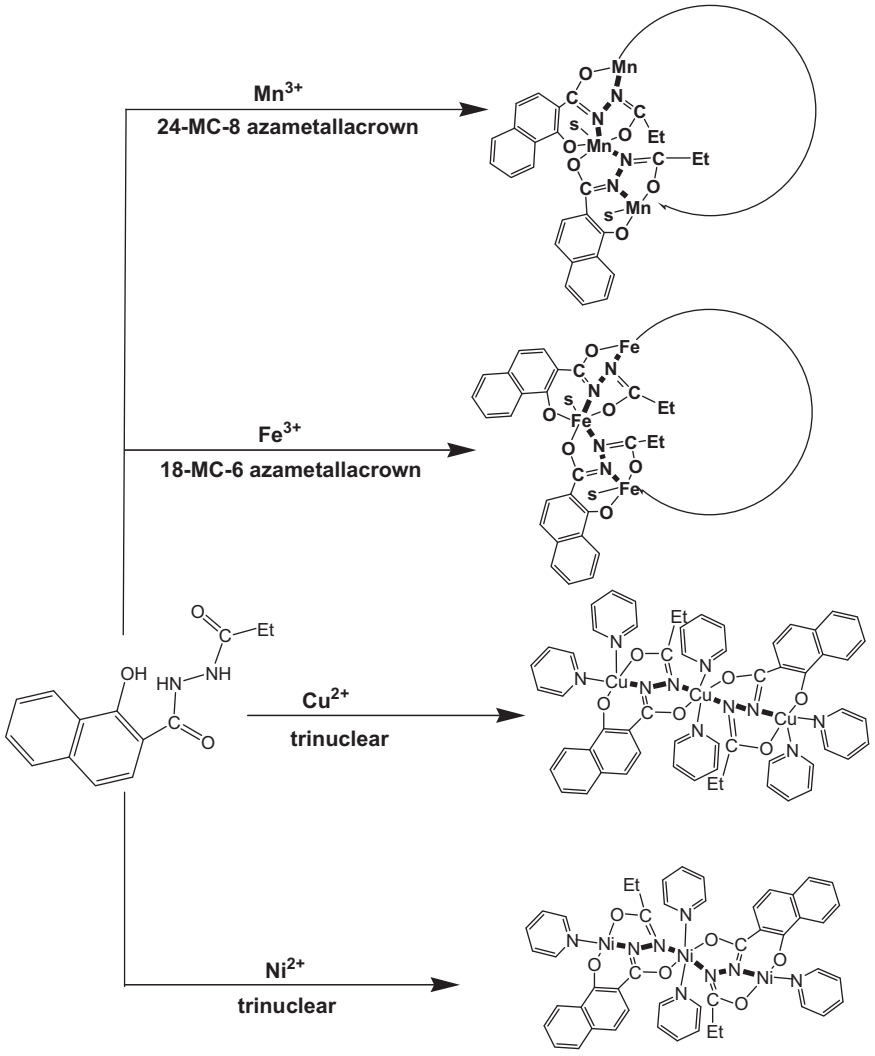

Scheme 1. Coordination architectures of the four complexes.

3.3. Magnetism

Temperature-dependent magnetic susceptibility measurements were performed on polycrystalline samples of the four complexes. Except for complex **4** with paramagnetic properties, other three complexes all exhibit antiferromagnetic coupling between the metal centers. In complexes **1**–**3**, there are three possible pathways of the coupling between two neighboring metal ions through the same ligand (two *M*–O–C–N–*M* and one *M*–N–N–*M*). We consider only one interaction (*J*) that will be the sum of these three couplings between the metal centers and the magnetic super-exchanges between the near-neighboring centers as well as those between the opposite centers were all omitted. The antiferromagnetic nature of the interaction can be understood

in terms of overlap through the bridging group between the single occupied metal *d*-orbitals.

The value of $\chi_M T$ for complex **1** is 23.99 emu mol^{-1} K at 300 K, close to the theoretical value of 24 emu mol^{-1} K for eight isolated high-spin Mn^{III} centers with $S=2$. Upon cooling, the value decrease steadily, reaching 14.19 emu mol^{-1} K at 25 K. Below this temperature, $\chi_M T$ decreased rapidly and reached 1.74 emu mol^{-1} K at 2 K. The antiferromagnetic coupling is further confirmed by a negative Weiss constant $\theta=-26.07$ K, which is calculated according to the Curie–Weiss law $\chi_M^{-1}(T)=C/(T-\theta)$ using the data within $T>25$ K. Assuming an idealized structure, the eight Mn(III) centers are simplified to be arranged in the symmetry of D_{8h}. The magnetic data were further fitted using MAGPACK package and the fitting results gave $g=2.03(3)$ and $J=-1.667$ K with $R=\sum[(\chi_M T)_{calc}-(\chi_M T)_{obs}]^2/\sum(\chi_M T)^2_{obs}=1.47\times10^{-5}$ as shown in the plot of $\chi_M T$ versus T in Fig. 9a (red line). All the values are consistent with other similar structures [25,56,57].

The magnetic data of complex **2** are shown in Fig. 9b. The value of $\chi_M T$ is 25.46 emu mol^{-1} K at 300 K, slightly smaller than the theoretical value of 26.25 emu mol^{-1} K for six noncoupling Fe(III) with $S=5/2$. The value steadily decreases to 10.54 emu mol^{-1} K at 50 K and then rapidly decreases and reaches 0.16 emu mol^{-1} K at 2 K. The fitting to the Curie–Weiss $\chi_M^{-1}(T)=C/(T-\theta)$ gave a negtive Weiss constant $\theta=-97.43$ K within $T>50$ K. The similar results have also been reported for other iron metalladiazamacrocycles [22,26]. Assuming the six Fe(III) centers arranged in the symmetry of D_{6h}, the data were fitted further to give $g=2.04(3)$ and $J=-2.297$ K with $R=\sum[(\chi_M T)_{calc}-(\chi_M T)_{obs}]^2/\sum(\chi_M T)^2_{obs}=3.14\times10^{-5}$ using MAGPACK package, as shown in the plot of $\chi_M T$ versus T in Fig. 9b (red line).

Fig. 9c shows the curve of the temperature dependence of the magnetic susceptibility (χ_M) and the inverse magnetic susceptibility (χ_M^{-1}) of complex **3**. The value of 1.22 emu mol^{-1} K of $\chi_M T$ at 300 K is slightly larger than the theoretical value 1.125 emu mol^{-1} K for three uncoupled Cu(II) centers with $S=1/2$. The $\chi_M T$ value decreases steadily till about 100 K and then decreases sharply to a value of 0.38 emu mol^{-1} K at 2 K. This fact indicates that antiferromagnetic coupling interaction exists between Cu(II) centers, mediated by the N–N diazine group, which is confirmed by a fitting to the Curie–Weiss $\chi_M^{-1}(T)=C/(T-\theta)$ with Weiss constant $\theta=-19.73$ K within $T>20$ K. And the data were fitted further using MAGPACK package to give $g=2.06(1)$ and $J=-13.68$ K with $R=\sum[(\chi_M T)_{calc}-(\chi_M T)_{obs}]^2/\sum(\chi_M T)^2_{obs}=1.67\times10^{-5}$ as shown in the plot of $\chi_M T$ versus T in Fig. 9c (red line), considering the linear arrangement of the Cu(II) ions within the trinuclear unit. The similar results have also been reported for other copper complexes [36].

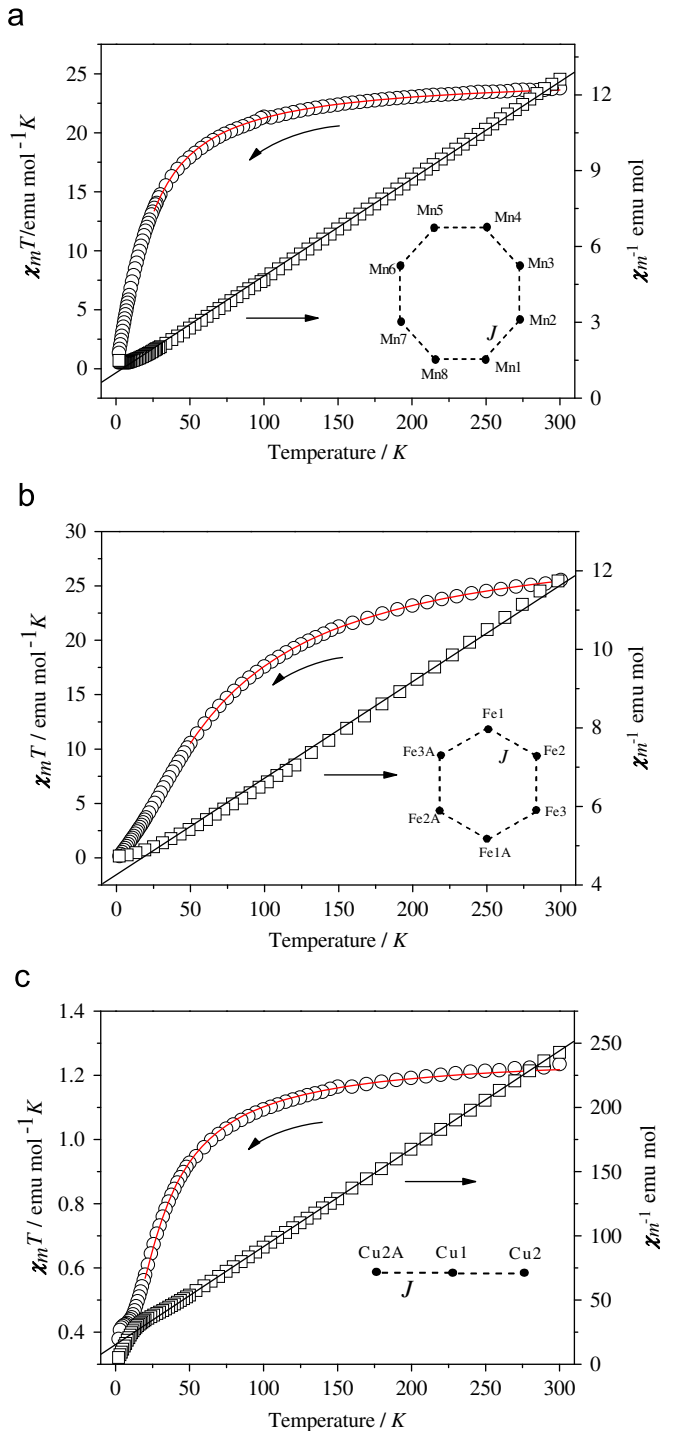

Fig. 9. Plots of the magnetic susceptibility $\chi_M T$ (round points) and the inverse magnetic susceptibility χ_M^{-1} (square points) versus temperature of complex **1**(a), complex **2**(b) and complex **3**(c), respectively. The lines represent the fitting curve according to the Curie–Weiss law and fitting using MAGPACK, respectively.

4. Conclusions

Based on N-substitued-1-hydroxy-2-naphthoylhydrazide ligand, we have obtained four complexes with different nuclearity from 24-membered octanuclear, 18-membered hexanuclear metalladiazamacrocycles to linear trinuclear complexes. This ligand acts as a pentadentate ligand and bridges metal ions in tridentate-bidentate fashion, forming metalladiazamacrocycles with trivalent metal ions and linear trinuclear complexes with bivalent metal ions, respectively. Complexes **1**, **2** and **3** all exhibit antiferromagnetic coupling interactions between the adjacent metal centers.

Supporting information available

CCDC 748519 (**1**), 748506 (**2**), 748514 (**3**), 748510 (**4**) contain the supplementary crystallographic data for complexes **1**–**4**, respectively. These data can be obtained free of charge via http://www.ccdc.cam.ac.uk/conts/retrieving.html. or from the Cambridge Crystallographic Data Centre, 12 Union Road, Cambridge CB2 1EZ, UK; fax: (+44) 1223 336 033; or e-mail: deposit@ccdc.cam.ac.uk.

Acknowledgments

We gratefully acknowledge financial support from the National Natural Science Foundation of China (Grant no. 20671048 and 20801025) and Taishan Scholar Fund.

Appendix A. Supporting information

Supplementary data associated with this article can be found in the online version at 10.1016/j.jssc.2010.07.021.

References

[1] B. Kwak, H. Rhee, S. Park, M.S. Lah, Inorg. Chem. 37 (1998) 3599.
[2] G. Mezei, C.M. Zaleski, V.L. Pecoraro, Chem. Rev. 107 (2007) 4933.
[3] M.S. Lah, V.L. Pecoraro, J. Am. Chem. Soc. 111 (1989) 7258.
[4] R.P. John, J. Park, D. Moon, K. Lee, M.S. Lah, Chem. Commun. (2006) 3699.
[5] A. Majumder, S. Goswami, S.R. Batten, M.S.E. Fallah, J. Ribas, S. Mitra, Inorg. Chim. Acta. 359 (2006) 2375.
[6] M. Moon, I. Kim, M.S. Lah, Inorg. Chem. 39 (2000) 2710.
[7] D. Moon, M.S. Lah, Inorg. Chem. 44 (2005) 1934.
[8] L.F. Jin, F.P. Xiao, G.Z. Cheng, Z.P. Ji, J. Organomet. Chem. 691 (2006) 2909.
[9] L.F. Jin, F.P. Xiao, G.Z. Cheng, Z.P. Ji, Inorg. Chem. Commun. 9 (2006) 758.
[10] F.P. Xiao, L.F. Jin, G.Z. Cheng, Z.P. Ji, Polyhedron 26 (2007) 2695.
[11] T.Y. Jiang, H.J. Zhong, T. Xiang, L.F. Jin, H. Yu, Inorg. Chim. Acta 362 (2009) 4729.
[12] T.P. Shu, Z.J. Chen, H.M. Feng, J.L. Wen, K.W. Lei, Inorg. Chem. Commun. 12 (2009) 672.
[13] X.F. Liu, W.L. Liu, K. Lee, M. Park, H.C. Ri, G.H. Kim, M.S. Lah, Dalton Trans. (2008) 6579.
[14] D. Moon, J. Song, B.J. Kim, B.J. Suh, M.S. Lah, Inorg. Chem. 43 (2004) 8230.
[15] M.J. Prakash, M.S. Lah, Chem. Commun. (2009) 3326.
[16] D. Moon, J. Song, M.S. Lah, CrystEngComm 11 (2009) 770.
[17] J. Choi, J. Park, M. Park, D. Moon, M.S. Lah, Eur. J. Inorg. Chem. (2008) 5465.
[18] B. Li, D.D. Han, G.Z. Cheng, Z.P. Ji, Inorg. Chem. Commun. 8 (2005) 216.
[19] J. Song, D. Moon, M.S. Lah, Bull. Korean Chem. Soc. 23 (2002) 708.
[20] R.P. John, K. Lee, M.S. Lah, Chem. Commun. (2004) 2660.
[21] S. Lin, S.X. Liu, Z. Chen, B.Z. Lin, S. Gao, Inorg. Chem. 43 (2004) 2222.
[22] S. Lin, S.X. Liu, J.Q. Huang, C.C. Lin, Dalton Trans. (2002) 1595.
[23] I. Kim, B. Kwak, M.S. Lah, Inorg. Chim. Acta. 317 (2001) 12.
[24] M. Park, R.P. John, D. Moon, K. Lee, G.H. Kim, M.S. Lah, J. Chem. Soc. Dalton Trans. (2007) 5412.
[25] R.P. John, K.J. Lee, B.J. Kim, B.J. Suh, H. Rhee, M.S. Lah, Inorg. Chem. 44 (2005) 7109.
[26] S.X. Liu, S. Lin, B.Z. Lin, C.C. Lin, J.Q. Huang, Angew. Chem. Int. Ed. 40 (2001) 1084.
[27] F.P. Xiao, L.F. Jin, Inorg. Chem. Commun. 11 (2008) 717.
[28] R.P. John, M. Park, D. Moon, K. Lee, S. Hong, Y. Zou, C.S. Hong, M.S. Lah, J. Am. Chem. Soc. 129 (2007) 14142.
[29] D. Moon, K. Lee, R.P. John, G.H. Kim, B.J. Suh, M.S. Lah, Inorg. Chem. 45 (2006) 7991.
[30] W.L. Liu, K. Lee, M. Park, R.P. John, D. Moon, Y. Zou, X.F. Liu, H.C. Ri, G.H. Kim, M.S. Lah, Inorg. Chem. 47 (2008) 8807.
[31] W. Luo, X.G. Meng, X.Z. Sun, F.P. Xiao, J.F. Shen, Y. Zhou, G.Z. Cheng, Z.P. Ji, Inorg. Chem. Commun. 10 (2007) 1351.
[32] C. Lin, M.X. Yang, S.X. Liu, Polyhedron 26 (2007) 4793.
[33] W. Luo, X.G. Meng, F.P. Xiao, G.Z. Cheng, Z.P. Ji, Polyhedron 27 (2008) 1802.
[34] W. Luo, X.T. Wang, G.Z. Cheng, S. Gao, Z.P. Ji, Inorg. Chem. Commun. 11 (2008) 769.
[35] W. Luo, X.G. Meng, G.Z. Cheng, Z.P. Ji, Inorg. Chim. Acta 362 (2009) 551.
[36] W. Luo, X.T. Wang, X.G. Meng, G.Z. Cheng, Z.P. Ji, Inorg. Chem. Commun. 11 (2008) 1044.
[37] L.F. Jin, L.J. Cheng, Inorg. Chim. Acta 361 (2008) 2109.
[38] K. Lee, R.P. John, M. Park, D. Moon, H.C. Ri, G.H. Kim, M.S. Lah, J. Chem. Soc. Dalton Trans. (2008) 131.
[39] J.M. Dou, M.L. Liu, D.C. Li, D.Q. Wang, Eur. J. Inorg. Chem. (2006) 4866.
[40] Y.T. Chen, J.M. Dou, D.C. Li, S.N. Wang, Inorg. Chem. Commun. 13 (2010) 167.
[41] G.M. Sheldrick, in: SADABS. Program for Empirical Absorption Correction of Area Detector Data, University of Göttingen, Germany, 1996.
[42] G.M. Sheldrick, in: SHELXL-97. Program for Crystal Structure Analysis, University of Göttingen, Germany, 1997.
[43] F.P. Xiao, L.F. Jin, W. Luo, G.Z. Cheng, Z.P. Ji, Inorg. Chim. Acta 360 (2007) 3341.
[44] L.F. Jin, H. Yu, S.X. Wu, F.P. Xiao, J. Chem. Soc., Dalton Trans. (2009) 197.
[45] S.N. Rao, K.N. Munshi, N.N. Rao, M.M. Bhadbhade, E. Suresh, Polyhedron 18 (1999) 2491.
[46] S. Holnes, C.J. Carrano, Inorg. Chem. 30 (1991) 1231.
[47] F.P. Xiao, L.F. Jin, Z. Anorg. Allg. Chem. 634 (2008) 397.
[48] F.P. Xiao, L.F. Jin, W. Luo, G.Z. Cheng, Z.P. Ji, Solid State Sci. 10 (2008) 1358.
[49] N.S. Biradar, A.L. Locker, J. Inorg. Nucl. Chem. 36 (1974) 1915.
[50] M.M. Bekheit, K.M. Ibrahim, Synth. React. Inorg. Met.-Org. Chem. 16 (1986) 1135.
[51] D. Coucouvanis, R.A. Reynolds, W.R. Dunham, J. Am. Chem. Soc. 117 (1995) 7570.
[52] M. Nishio, Cryst. Eng. Comm 6 (2004) 130.
[53] Y.T. Wang, G.M. Tang, W.Y. Ma, W.Z. Wan, Polyhedron 26 (2007) 782.
[54] E. Bilewicz, A.J. Rybarczyk-Pirek, A.T. Dubis, S.J. Grabowski, J. Mol. Struct. 829 (2007) 208.
[55] I. Kim, B. Kwak, M.S. Lah, Inorg. Chim. Acta 317 (2001) 12.
[56] B. Kwak, H. Rhee, M.S. Lah, Polyhedron 19 (2000) 1985.
[57] Z.J. Chen, Inorg. Chem. Commun. 12 (2009) 636.
[58] W. Luo, X.T. Wang, X.G. Meng, G.Z. Cheng, Z.P. Ji, Polyhedron 28 (2009) 300.